Anti-Folate Receptor alpha–directed Antibody Therapies Restrict the Growth of Triple Negative Breast Cancer

Anthony Cheung[1,2], James Opzoomer[1,2], Kristina M Ilieva[1,2], Patrycja Gazinska[1], Ricarda M Hoffmann[2], Hasan Mirza[1], Rebecca Marlow[1], Erika Francesch-Domenech[1], Matthew Fittall[1,2], Diana Dominguez Rodriguez[1,2], Angela Clifford[1], Luned Badder[1], Nirmesh Patel[1], Silvia Mele[2], Giulia Pellizzari[2], Heather J Bax[2,3], Silvia Crescioli[2], Gyula Petranyi[2], Daniel Larcombe-Young[1], Debra H Josephs[2,3], Silvana Canevari[4], Mariangela Figini[4], Sarah Pinder[3,5], Frank O Nestle[6,2], Cheryl Gillett[3,5], James F Spicer[3], Anita Grigoriadis[1], Andrew N J Tutt[1,7] and Sophia N Karagiannis[1,2]

[1] Breast Cancer Now Research Unit, School of Cancer & Pharmaceutical Sciences, King's College London, Guy's Cancer Centre, London, United Kingdom;
[2] St. John's Institute of Dermatology, School of Basic & Medical Biosciences, King's College London, & NIHR Biomedical Research Centre at Guy's and St. Thomas' Hospitals and King's College London, Guy's Hospital, King's College London, London, United Kingdom;
[3] School of Cancer & Pharmaceutical Sciences, King's College London, Guy's Cancer Centre, London, United Kingdom;
[4] Department of Applied Research and Technology Development, Fondazione, IRCCS Istituto Nazionale dei Tumori Milano, 20133, Milan, Italy;
[5] King's Health Partners Cancer Biobank, King's College London, London, United Kingdom;
[6] Immunology and Inflammation Therapeutic Research Area, Sanofi US, Cambridge, Massachusetts, USA;
[7] Breast Cancer Now Toby Robins Research Centre, Institute of Cancer Research, London, United Kingdom

Running title:
Anti-FRα antibody against triple negative breast cancers

Correspondence: Sophia N. Karagiannis, PhD, St. John's Institute of Dermatology, School of Basic & Medical Biosciences, King's College London & NIHR Biomedical Research Centre at Guy's and St. Thomas's Hospitals and King's College London, Guy's Hospital, Tower Wing, 9th Floor, London, SE1 9RT, UK; Tel: +44(0)20 7188 6355; E-mail: sophia.karagiannis@kcl.ac.uk

Disclosure of Potential Conflicts of Interest
S.N. Karagiannis and J.F. Spicer are founders and shareholders of IGEM Therapeutics Ltd. F.O. Nestle is an employee of Sanofi US. All other authors have declared that no conflict of interest exists.

1

Translational Relevance

Triple negative breast cancer (TNBC) represents a molecularly and clinically diverse disease with cytotoxic chemotherapy the only systemic treatment modality, and no targeted agents approved in adjuvant, neoadjuvant, or metastatic settings. We demonstrate that a significant population of aggressive high-grade TNBCs overexpress the cell surface tumor-associated antigen Folate Receptor alpha (FRα) and molecules involved in folate metabolism. Importantly, FRα is expressed in post-neoadjuvant chemotherapy residual disease, associated with worse clinical outcomes, and participates in cancer cell signaling and growth. We show that FRα may present a promising target for therapeutic strategies such as antibody-drug conjugates, or antibody immunotherapy that primes an Fc-mediated anti-tumor immune response *in vitro* and *in vivo* in the human patient breast cancer and the patient immune context. Engineering antibodies targeting FRα-expressing breast cancers may provide new strategies to treat patients with poor prognosis who do not adequately benefit from currently-available targeted, and immuno-oncology therapies.

Abstract

3

Purpose: Highly-aggressive triple negative breast cancers (TNBCs) lack validated therapeutic targets and have high risk of metastatic disease. Folate Receptor alpha (FRα) is a central mediator of cell growth regulation that could serve as an important target for cancer therapy.

Experimental Design: We evaluated FRα expression in breast cancers by genomic (N = 3414) and immunohistochemical (N = 323) analyses and its association with clinical parameters and outcomes. We measured the functional contributions of FRα in TNBC biology by RNA interference and the anti-tumor functions of an antibody recognizing FRα (MOv18-IgG1), *in vitro* and in human TNBC xenograft models.

Results: FRα is overexpressed in significant proportions of aggressive basal like/TNBC tumors, and in post-neoadjuvant chemotherapy-residual disease associated with a high risk of relapse. Expression is associated with worse overall survival. TNBCs show dysregulated expression of thymidylate synthase, folate hydrolase 1 and methylenetetrahydrofolate reductase, involved in folate metabolism. RNA interference to deplete FRα decreased Src and ERK signaling and resulted in reduction of cell growth. An anti-FRα antibody (MOv18-IgG1) conjugated with a Src inhibitor significantly restricted TNBC xenograft growth. Moreover, MOv18-IgG1 triggered immune-dependent cancer cell death *in vitro* by human volunteer and breast cancer patient immune cells, and significantly restricted orthotopic and patient-derived xenograft growth.

Conclusions: FRα is overexpressed in high-grade TNBC and post-chemotherapy residual tumors. It participates in cancer cell signaling and presents a promising target for therapeutic strategies such as antibody-drug conjugates, or passive immunotherapy priming Fc-mediated anti-tumor immune cell responses.

Introduction

Triple negative breast cancer (TNBC), defined by lack of oestrogen receptor (ER), progesterone receptor (PR) and human epidermal growth factor receptor 2 (HER2) expression, represents an urgent unmet clinical need for treatment options. This is largely due to its aggressive nature and lack of suitable therapeutic targets. TNBC is a heterogeneous disease at the cellular and molecular levels, with its diverse phenotypes correlating with different drug resistance and clinical outcomes (1). Gene expression profiling and expression signatures have identified five molecularly-distinct types of breast cancers, including ER-positive luminal (luminal A and B), HER2-positive, normal-like and basal-like (BL) subtypes. The majority of BL carcinomas have a high mitotic rate, and are usually triple-negative (2). Different TNBC subgroups also correlate with risk factors, incidence, prognosis and treatment response (3). The Lehman-Pietenpol expression classification crystallizes six further TNBC subtypes with implications for prediction of prognosis and chemotherapy sensitivity (4). Although TNBCs are largely defined by a clinical diagnosis of exclusion based on pathological parameters, together these studies point to the potential for identification of disease-associated markers which may serve to define patient subgroups and lead to personalized targeted therapy.

At present, no targeted treatments are standard of care for TNBC. Antibodies recognizing growth factor receptors such as cetuximab or bevacizumab (5, 6), and small molecule drugs such as dovitinib and cabozantinib (7, 8), have been explored in clinical trials, alone or in combination with chemotherapy. These have shown relatively limited response rates in unselected patient populations (9), most likely due to activation of alternative compensatory pathways and inter-/intra-tumoral heterogeneity in expression and mutational status, which may be responsible for intrinsic and acquired resistance-driving mechanisms (10). Thus, disease management mostly relies on a combination of surgery, radiotherapy and multiple chemotherapeutic agents, often associated with high risk of local and systemic relapse (11).

Folate Receptor alpha (FRα) and its ligand folate are central mediators of cell growth regulation for the one-carbon metabolic reaction and DNA biosynthesis, repair and methylation (12). Insights into FRα distribution (high expression in tumors and restricted expression in normal tissues), alongside emerging roles in cancer growth and metastasis have led to renewed interest in this as a therapy target (13, 14). Preclinical and clinical anti-tumor activities of FRα-targeted therapies have thus far mostly been examined in the context of lung and ovarian carcinomas. These include monoclonal antibodies

4

farletuzumab (15) and MOv18-IgG1 (16), antibody-drug conjugate (ADC) Mirvetuximab Soravtansine (17), and small molecule drug vintafolide (18). Encouraging results have recently been reported for the thymidylate synthase inhibitor ONX-0801 in ovarian carcinoma (19). The FRα-targeted hapten immunotherapeutic regimen, Folate Immune, was designed to render tumors more immunogenic; however, a phase II trial in renal carcinoma was terminated due to low patient accrual (NCT00485563). Another phase I trial of a FRα-specific chimeric antigen receptor (CAR)-T cell therapy in ovarian cancer patients showed no reduction in tumor burden (20). Recently, Song *et al.* showed that new generation FRα-specific CAR-T cells significantly inhibited high FRα-expressing TNBC xenograft growth (21). However, monoclonal antibody therapeutics agents targeting FRα are yet untested in TNBC.

In this study, we examined FRα as a target for monoclonal antibody therapy approaches. We ascertained the clinical and biological significance of FRα in TNBC and the largely overlapping basal-like subtype, associations of FRα expression with clinical parameters and outcomes by genomic and immunohistochemical analyses. We employed RNA interference and cell-based functional assays to interrogate how FRα may contribute to breast cancer cell biology. We studied FRα and its downstream folate pathway as therapeutic targets by assessing the potential anti-tumor functions of an antibody recognizing FRα (MOv18-IgG1); as an ADC to inhibit cellular viability *in vitro* and tumor growth *in vivo*; and as immunotherapy to activate human immune cells against TNBC *in vitro*, in orthotopic and patient-derived tumor xenografts (PDTX) *in vivo,* more likely able to recapitulate the complexity and heterogeneity of human disease (22). Our findings define FRα as a promising target for antibody therapies for basal-like breast carcinomas including TNBCs.

5

Materials and Methods

Cell lines

Cell lines were obtained from King's College London (KCL) Breast Cancer Now Unit, except HDQ-P1, purchased from Leibniz Institute DSMZ. Cell lines were authenticated by short tandem repeat profiling. Cells used once tested negative for mycoplasma and used up to 30 passages.

Gene expression data of human breast cancers

The KCL Guy's Hospital, METABRIC and TCGA Breast cohorts (N=2012) interrogated were previously reported (23, 24, 25). Statistical analyses and respective data plots were generated in R version 3.2.2.

Tissue microarray (TMA) and immunohistochemistry (IHC)

Primary breast carcinomas from 305 patients with no prior neoadjuvant therapy, and 18 surgical specimens from TNBC post-neoadjuvant chemotherapy (post-NACT) residual cancer burden II/III residual cases were evaluated. Access to pseudo-anonymized samples and clinical data were obtained in accordance with the terms and conditions of National Health Service Research Ethics Committee approved Guy's and St Thomas' Research Tissue and Data Bank (REC No 07/H0804/131). PDTX TMA collection included 26 TNBC tumors obtained by directly implanting patient material orthotopically into NSG mouse mammary fat pads. Staining was performed with FRα IHC Kit (BioCare Medical) following manufacturer's protocol, with additional 30 min anti-FRα incubation (API3005AA). IHC with CD45 (Thermo Fisher Scientific) was detected using the DAKO EnVision System HRP Kit (peroxidase activity visualized with 3,3-diaminobenzidine). Analyses were performed using digital images by NanoZoomer HT Digital Pathology Scanning System (Hamamatsu).

siRNA- and lentiviral-mediated RNA interference

FRα-targeting siRNA sequences and scrambled duplex were purchased from OriGene. Transient transfection was performed using Lipofectamine2000 (Thermo Fisher Scientific). Viral particles of Tet-pLKO-puro plasmid encoding FRα-specific (5'-GGATGTTTCCTACCTATATAGATTC), and non-targeting sequence (5'-GCGCGATAGCGCTAATAATTT) were generated by transfection into 293T cells. CAL51

6

were transduced using 1:30 viral dilution of isolated viral supernatant. Successfully transduced clones were selected after 48 hr with 3 µg/ml of puromycin for 5 days, and 1 µg/ml of doxycycline was used to induce FRα knockdown.

In vitro viability and clonogenic assay

Cell viabilities were detected by methyl tetrazolium assay (Promega). Optical absorbance was read on FLUOstar Omega spectrophotometer (BMG Labtech) to determine viable cell counts after 96 hr. For clonogenic assays, cells were fixed by methanol, stained with crystal violet solution (Sigma Aldrich). Colonies were measured as a function of mean pixel density per well. Image analysis was performed using ImageJ.

Western blot and Human Phospho-Kinase Antibody Array

Immunoblottings were analyzed with anti-phospho-ERK1/2 (Thr202/Tyr04) (Biolegend) and anti-ERK1/2 (Cell Signalling). Proteome Profiler Human Phospho-Kinase Antibody Array (R&D Systems) were incubated with 470 µg lysate overnight at 4°C. The following day, chemiluminescent detection was done according to manufacturer's protocols. Densitometry analysis was performed using ImageJ.

Antibody-drug conjugate production

MOv18-IgG1 was linked to streptavidin overnight using Lightning-Link Streptavidin Conjugation Kit (Expedeon) according to manufacturer's protocol. A-419259 (Cayman Chemical) was biotinylated using EZ-Link-Sulfo-NHS-Biotin (Thermo Fisher Scientific): 10 mM solution in PBS added to 10 mM EZ-Link-Sulfo-NHS-Biotin in ultrapure water (molar ratio 8:1), incubated at room temperature for 30 min, 133 µl of 1.1 mM solution of biotinylated A-419259 was added per 1 mg of streptavidin-conjugated MOv18-IgG1, followed by 30 min incubation. The ADC was purified by centrifugation using 3K Amicon ultra centrifugal filters six times, then resuspended in PBS for functional experiments.

Fluorescence-based tumor cell killing assays

For live-dead cell cytotoxicity imaging, cancer cells were stained with 5 µM CFSE (Life Technologies). The following day, human peripheral blood mononuclear cells (PBMCs) were isolated using Ficoll Paque PLUS (GE Healthcare) and stained with CellTracker Blue dye (Thermo Fisher Scientific). PBMCs were incubated with cancer cells and MOv18-IgG1

7

or isotype antibody. Ethidium homodimer-1 (4 µM) (Thermo Fisher Scientific) served to label dead cells. Samples were imaged using Eclipse Ti-2 inverted microscope equipped with Nikon DS-Qi2 sCMOS camera and running NIS Elements. Antibody-dependent cell-mediated killing of tumor cells was quantified as previously described (26). Data were acquired using FACSCanto flow cytometer (BD Biosciences).

In vivo procedures

Animals were handled in accordance with Institutional Committees on Animal Welfare (The Home Office Animals Scientific Procedures Act, 1986). Antibody-drug conjugate: Six-week-old female CD-1 nude mice were used for orthotopic injection of 1×10^6 CAL51 cells (50 µl PBS mixed in 50 µl Matrigel) (day 1). On day 5, mice received single intravenous injection of 7.5 mg/kg ADC or MOv18-IgG1, or 5 mg/kg A-419259. Tumors were measured with calipers and volumes calculated ($\pi \times$ length $\times$ width^2 / 6). Experiments were terminated after 28 days when tumor sizes were ≤ 525 mm^3. Antibody immunotherapy: Female NSG mice were orthotopically injected with 1×10^6 CAL51 cells or 0.25×10^6 WHIM02 PDTX single cell digests in 50 µl PBS:50 µl Matrigel (day 1). For CAL51, on days 5 and 19, each mouse received 12×10^6 human peripheral blood lymphocytes (PBLs) (following red blood cell lysis of human blood) intravenously and 5 or 10 mg/kg MOv18-IgG1. Subsequent antibody was given once per week. For WHIM02, on days 5 and 18, 12×10^6 human PBLs and 10 mg/kg antibody per mouse were given intravenously. Antibody doses were given three times in week one and subsequently twice per week. Experiments were terminated after 33 days for CAL51 and 20 days for WHIM02, and tumor sizes were ≤ 525 mm^3. Tumor engraftment of human immune cells was confirmed by IHC staining and flow cytometry (antibody panel: rat anti-mouse CD45-V500; mouse anti-human CD45-PE-Cy7, CD20-APC, CD3-APC-Cy7, CD68-PE (all BD Biosciences), CD14-PE (eBioscience), CD56-PercP Cy5.5 (Cambridge Bioscience).

Statistical analyses

GraphPad Prism was used for statistical analyses. Data were presented as mean ± standard error of the mean (SEM). Differences with *P*-values < 0.05 were considered statistically significant and all tests were two-sided.

Please see Supplementary Experimental Procedures for more detailed methods.

Results

Gene expression pattern of FRα reveal associations with TNBC and basal-like breast cancer

We investigated whether FRα (*FOLR1*) is expressed in TNBC and its majority basal-like subtype by interrogating three transcriptomic datasets: METABRIC (N = 1197) (25), The Cancer Genome Atlas (TCGA) (N = 638) (24) and the KCL TNBC-enriched cohort (N = 177) (23). When tumors were stratified by IHC-defined status, *FOLR1* levels were significantly higher in TNBC compared with non-TNBC (Fig. 1A). *FOLR1* expression was also higher in the basal-like molecular subtype defined by PAM50 classification (Fig 1B). The small changes of DNA copy number in the genome suggest that copy number had an insignificant impact on *FOLR1* expression (Supplementary Fig. 1A). *FOLR1* was expressed in all TNBC subtypes as classified by the Lehman-Pietenpol method (Supplementary Fig. 1B).

Although plasma folate levels have not been clearly associated with breast cancer risk (27), low folate status can lead to hypomethylation, subsequent dysregulation of one-carbon metabolism and DNA instability. This may in turn influence the levels of folate receptors or folate carriers (28). However, the association between breast cancer and folate status in the tumor microenvironment remains undetermined. We investigated three molecules involved in folate metabolism that may be of therapeutic interest in cancer. We found that mRNA levels of methylenetetrahydrofolate reductase (*MTHFR*), a key enzyme in the folate metabolic pathway, are significantly decreased in METABRIC and TCGA cohorts, although not in the KCL dataset (possibly due to enriched TNBC and low non-TNBC patient tumor groups). Furthermore, Thymidylate Synthase *(TYMS)*, a folate-dependent enzyme involved in the biosynthesis of thymidine for DNA synthesis and repair (29), was upregulated in all datasets. There was no significant correlation between *FOLR1* and *MTHFR* or *TYMS* expression, suggesting that FRα and folate carriers may be independently-regulated in tumors. Notably, expression of folate hydrolase 1 (*FOLH1*, also known as prostate specific membrane antigen (*PSMA*)), a transmembrane folate hydrolase overexpressed in prostate and breast cancers (30), was higher in TNBC/basal-like subtypes. We found a weak correlation between *FOLH1* with *FOLR1* expression (Pearson's *r* = 0.31, *p < 0.0005*) (Fig. 1C), perhaps suggesting collaborative roles in the tumor microenvironment.

9

Furthermore, the ten-year overall survival (OS) of patients with high FRα tumor expression was significantly lower than those with medium/low expression (Hazard Ratio (HR) = 1.38, P = 0.0097) in all breast cancers (N = 1402) (Fig. 1Di). Survival analysis of the TNBC patient subset revealed that despite small cohort size (N = 47), high FRα expression correlated with decreased OS (HR = 3.35, P = 0.043) (Fig. 1Dii).

Thus, elevated FRα gene expression and dysregulated expression of molecules involved in folate metabolism were detected in basal-like breast carcinomas including TNBCs, and FRα expression was associated with worse patient outcomes.

FRα membrane expression by immunohistochemical evaluations

We next examined FRα expression on a cross-sectional study of breast carcinoma TMA specimens (N = 323, of which 76 were TNBCs) (Fig. 2A). In contrast to a restricted distribution pattern in normal tissues (31), high frequency (>70%) FRα protein expression correlated with high grade disease (Grade I: 0.0%; II: 7.7%; III: 24.7%). Three quarters of the FRα-positive grade III samples displayed a medium (41-70%) or a high (71-100%) percentage of cancer cells with membrane FRα immunostaining. Expression was less frequently-associated with ER-positive (7.5%), HER2 (15.6%) or luminal (6.5%) tumors, relative to ER-negative tumors (30.0%) and TNBC (36.8%) (by IHC classification). FRα expression in TNBCs vary among studies, from 20% (32) to 67% or 80% positivity (33, 34). According to PAM50 molecular classification, we observed FRα expression in 10.7% of HER2-positive and 7.1% of luminal A cancers, while FRα expression was more common in basal-like subtypes (33.3%) (Supplementary Table 1) in concordance with a recent report (32). Furthermore, cell membrane FRα immunostaining, significantly correlated with mRNA expression in the same patient samples (P < 0.0005) (Fig. 2B). We also found that 13% of samples negative for membrane FRα demonstrated cytoplasmic, non-membrane, FRα staining; these tissues may not be amenable to anti-FRα antibody treatment.

Due to lack of effective targetable oncogenic drivers, treatment for TNBC commonly involves cytotoxic chemotherapy, often given prior to surgery. A subpopulation of chemotherapy-resistant residual tumor cells remaining in breast tissue may be responsible for high metastatic recurrence rates and poor long-term clinical outcomes (35, 36). In a TMA containing eighteen TNBC samples from patients with residual disease post-NACT, we found FRα expression in 61.1% of residual tumors (Fig. 2C), and >75% of positive

10

samples displayed medium or high percentage of cells with membrane FRα immunostaining.

In summary, more TNBC specimens have FRα-positive immunostaining than other breast cancer subtypes. This is particularly marked in post-NACT residual disease, suggesting that FRα could be therapeutically targeted.

FRα expression contributes to breast cancer growth

To gain insights into FRα functions, we evaluated FRα expression in twenty-two breast cancer cell lines by flow cytometry using the monoclonal antibody MOv18-IgG1 (Fig. 3A, Supplementary Fig. 2A-C). Protein expression correlated with transcriptomic expression (Cancer Cell Line Encyclopedia (CCLE)) (Spearman's rank coefficient, $r = 0.5784$, $P < 0.01$, Fig. 3B). Three cell lines (CAL51, T47D and HDQ-P1) showed the highest levels of FRα expression by mRNA and corresponding cell surface expression.

Traditionally FRα has been viewed as an intracellular transporter of soluble folate. However, recent findings indicate that FRα may form macromolecular complexes in which it may contribute to upregulation of oncogenic STAT3/JAK pathways (37) and Lyn signaling (38). We therefore hypothesized that FRα expression may confer a proliferative advantage to high-expressing tumors. Employing RNA interference, we found that FRα expression (mean fluorescence intensity, MFI) in cells treated with FRα-targeting siRNA (siFRα) was significantly lower than in those treated with non-targeting siRNA (siNT) (Supplementary Fig. 2D). Reduction in FRα was accompanied by reduced cell viability compared with scrambled siRNA-treated cells (Fig. 3C, Supplementary Fig. 2E). FRα knockdown also resulted in reduction of colony formation (Fig. 3C, Supplementary Fig. 2F). Neither viability nor colony formation were affected by FRα knockdown in low FRα-expressing MDA-MB-231 cells.

To further interrogate the contribution of FRα to breast cancer biology, we created a stable, doxycycline-inducible, FRα-knockdown CAL51 cell line. The resulting shRNA-transduced cells had a four-fold lower mean relative FRα expression measured by flow cytometry when compared with cells transduced with non-targeting sequence (shNT). In concordance with siRNA experiments, FRα knockdown led to a modest reduction in proliferation (to 75.9 ± 2.2% viability (% ± SEM: $P < 0.0005$), and reduced colony formation ability (to 65.8 ± 23.1%, $P < 0.05$). Furthermore, consistent with proposed roles in downstream oncogenic signaling pathways such as STAT3/JAK, we measured a

11

significant decrease in phosphorylated ERK activity to 30.4 ± 7.2% ($P < 0.0005$) with FRα knockdown, suggesting reduction of another proliferative signaling pathway (Fig. 3D, Supplementary Fig. 3A).

Furthermore, we studied the anti-tumor effects of raltitrexed, a highly-selective inhibitor of thymidylate synthase, the key enzyme in folate metabolism (Fig. 1). CAL51 shNT cells (with high FRα expression levels) were more sensitive to raltitrexed compared to FRα-knockdown cells in both normal or folate-free conditions (Fig. 3E).

Together, these data indicate that FRα plays key roles in cell growth and TNBC may be sensitive to therapeutic treatment targeting the folate cycle.

FRα-dependent signaling functions in breast cancer cells

We sought to interrogate the molecular signaling processes regulated by FRα and explore the development of targeted therapeutic options. Signaling pathways were assessed using a human phosphokinase array studied in shNT- and shFRα-transduced CAL51 (Fig. 4A). FRα knockdown significantly decreased the activity of several members of the Src-family non-receptor tyrosine kinase, Lyn, Fyn, Hck and Src, their downstream effector molecule ERK, and of the anti-apoptotic protein CREB. Moreover, FRα silencing was associated with increased activity of the metabolic regulator AMPKa1 and the cell cycle regulator p53 (S15 and S392), when compared with control shRNA treatment.

Growth inhibition by the broad spectrum Src-family kinase inhibitor A-419259 was observed in cell lines with high FRα expression, but not with MDA-MB-231 which express near background levels of FRα (Fig. 4B). Growth inhibition was also demonstrated in CAL51 using a second Src-family kinase inhibitor AZM475271 (Supplementary Fig. 3C). The A-419259 inhibitor (50nM) also significantly reduced colony formation to 31.2 ± 4% ($P < 0.0005$) and ERK activation to 54.6 ± 9.2% ($P < 0.005$) (Fig. 4B).

These data suggest that FRα is upstream of multiple Src-family kinases and ERK (Fig. 4C), known to be involved in breast cancer biology, and identify FRα as cell surface molecule associated with signaling and growth, with potential to be targeted in therapeutic strategies for TNBC.

The anti-FRα antibody MOv18-IgG1 exerted a very modest direct inhibition in cell viability under folate-reduced conditions (0.4nM folate) (remaining viability: 86.3 ± 2.5%, $P < 0.05$ for 10 μg/ml; 87.5 ± 0.9%, $P < 0.005$ for 50 μg/ml), when compared with media alone

controls (Supplementary Fig. 3D). This suggested that any direct anti-tumor effects of these agents may be limited to folate-depleted environments, perhaps akin to conditions found in tumors.

MOv18-IgG1 did not engender significant direct inhibition of FRα-dependent signaling under physiological conditions. We therefore developed a FRα-targeting antibody-coupled inhibitor ADC strategy by conjugating the Src-family kinase inhibitor A-419259 to MOv18-IgG1, using the antibody as a vehicle to specifically deliver the inhibitor to cancer cells. Cell viability assessments resulted in significantly-lower IC_{50} dose for ADC (0.47 nM) compared with inhibitor alone treatment (>50 nM) (Fig. 4D). In CAL51 xenografts, ADC or A-419259 treatment resulted in significantly-reduced tumor growth and tumor weights compared with antibody alone or vehicle controls. ADC resulted in significantly-lower tumor weights (14.7 ± 1.4, mg ± SEM) compared with vehicle (32.5 ± 2.4 mg, $P < 0.0005$) or antibody (39.4 ± 8.8 mg, $P < 0.005$) treatments. Tumor weights after inhibitor treatment (19.9 ± 5.0 mg) were significantly-lower than antibody or vehicle controls ($P < 0.05$). ADC (7.5 mg/kg, equivalent to 2.66 μg A-419259 per mouse) and inhibitor alone (5 mg/kg, equivalent to 0.1 mg A-419259 per mouse) showed similar growth inhibition, although the A-419259 dose coupled with ADC measured only 2.66% of the dose of uncoupled inhibitor (Fig. 4E).

Our findings demonstrate the therapeutic potential of ADC targeting FRα and downstream pathways against breast cancer.

MOv18-IgG1 induces tumor cell killing by human immune cells

We next evaluated the potential of MOv18-IgG1 to activate immune effector cells against cancer cells. In a live-dead cell cytotoxicity imaging assay, human PBMCs pre-labeled with CellTracker Blue dye served as immune effector cells, and CFSE-labelled CAL51 were used as targets. We observed higher rates of dead cells (red fluorescent cells, depicting ethidium homodimer-1 incorporation into dead cells) with MOv18-IgG1 compared with control antibody treatments (Fig. 5A). We quantified tumor cell killing (Antibody-Dependent Cell-mediated Cytotoxicity (ADCC) and Phagocytosis (ADCP)) by MOv18-IgG1 using a flow cytometry-based assay (26). With U937 human monocytes as effector cells (Supplementary Fig. 4A), MOv18-IgG1 mediated killing of FRα-expressing, but not of low FRα-expressing cancer cells by a combination of ADCC and ADCP functions (Fig. 5B; Supplementary Fig. 4C). MOv18-IgG1 induced predominantly ADCP effects (ADCC vs

13

ADCP ratios: CAL51 = 1.6:1, T47D = 0.4:1, HDQ-P1 = 0.5:1). These effector functions are consistent with previously-reported tumor cell killing engendered by human monocytes and tumor antigen-specific IgG1 antibodies (26, 39).

Breast cancer patients' immune responses may be suppressed, and patient immune profiles may be altered by adjuvant radiotherapy or chemotherapy (40), hence potentially less capable of restricting tumor growth. MOv18-IgG1 could stimulate immune effector cells (PBMC) from healthy volunteers and patients with TNBC (patient characteristics: Supplementary Fig. 4D) to kill CAL51 in an antigen-specific manner (ADCC vs ADCP ratio: healthy volunteers 0.8:1; TNBC patients 0.7:1) (Fig. 5C, Supplementary Fig. 4E and 4F).

These data demonstrate the ability of an anti-FRα antibody to activate patient immune effector cells to induce breast cancer cell death *in vitro.*

Anti-FRα antibody treatment restricts the growth of two orthotopic TNBC human xenograft tumors *in vivo*

We examined the potential Fc-mediated anti-tumor effects of MOv18-IgG1 *in vivo*. We employed an orthotopic mammary fat pad-established human TNBC xenograft in immunodeficient mice. This model features impairments in B, T and natural killer (NK) cell development and functions, and lack MHC class I/II expression, designed to minimize the xenogeneic graft-versus-host disease. The model allows introduction of human immune cells to serve as human FcR-expressing effector cells (41), therefore, treatments followed introduction of immune effector cells (freshly-isolated human PBL).

Immunohistochemical evaluations of established xenografts confirmed *in situ* FRα expression in mammary orthotopically-formed CAL51 tumors (Fig. 6A). Tumors from mice given PBL showed human immune cell (CD45^{+}) infiltration in immunohistochemical evaluations (Fig. 6B), confirmed by flow cytometric assessments of human CD45^{+} cells extracted from xenografts. MOv18-IgG1-treated animals at either 5 or 10 mg/kg dosages showed significantly reduced tumor growth and resected tumor weights (Fig. 6C) compared with controls. Average tumor weight was 90 ± 20 (mg ± SEM) for the 5 mg/kg group and 60 ± 10 mg for the 10 mg/kg group, compared to control mice given PBS (150 ± 20 mg, *P* < 0.05), PBL-alone (120 ± 10 mg, *P* < 0.005) or antibody-alone (170 ± 20 mg, *P* < 0.005).

We investigated whether the antibody treatment could also restrict TNBC PDTX growth. Immunohistochemical evaluations revealed that 11 of 26 (46.2%) PDTX tumors were FRα

14

positive (Fig. 6D). We examined the efficacy of MOv18-IgG1 in the fast-growing WHIM02 PDTX model that features high (100% of cells) membrane FRα expression. All WHIM02 tumors injected with PBL showed immune cell infiltration in tumor stroma irrespective of treatment (Fig. 6E). Average tumor weight was 350 ± 40 mg in PBL-alone group compared to 100 ± 20 mg with MOv18-IgG1 treatment (71% lower average tumor weight, *P* < 0.0005), suggesting significantly-reduced growth associated with antibody treatment. Although the great proportion of infiltrating CD45$^+$ human cells were T cells (Supplementary Fig. 5), we measured a modest increase in tumor-infiltrating macrophages (3.8 ± 0.9% with MOv18-IgG1, compared to 1.2 ± 0.5% PBS, *P* < 0.05) and NK cells (5.7 ± 1.5% with MOv18-IgG1, compared to 1.7± 0.5% PBS, *P* < 0.05) (Fig. 6G) associated with antibody treatment. This is consistent with the immune activation seen *in vitro*.

Our results therefore demonstrate significant tumor growth restriction associated with anti-FRα antibody in both orthotopic TNBC line and PTDX models. These effects may at least partly be attributed to a responsive, antibody-dependent, immune effector cell mechanism, a notion supported by MOv18-IgG1-mediated tumor/immune cell interactions and ADCC/ADCP functions against cancer cells.

15

Discussion

Cytotoxic chemotherapy remains the only systemic treatment modality for patients with TNBC, partly because tumor-associated molecules amenable to targeted therapies including antibodies need to be identified and validated. Our genomic and immunohistochemical evaluations demonstrate that a significant population of TNBCs, including viable post-neoadjuvant chemotherapy residual disease, are likely to overexpress the tumor-associated antigen FRα, and that this antigen participates in the biological functions of breast cancer cells. We show that monoclonal antibody approaches recognizing FRα can offer treatment strategies against TNBC, such as through the design of an antibody conjugate to specifically deliver a signaling blocking agent (Fig. 4).

Avoiding immune destruction is considered a hallmark of cancer (42), yet recent breakthroughs demonstrate that the immune system can play important roles in controlling malignant disease, and that antibodies can provide a means by which immune cells could be directed against cancer. For example, treatment with anti-PD-1 inhibitor antibody pembrolizumab could confer clinical responses in 18.5% of patients with advanced TNBC pre-screened for expression of the ligand PD-L1 in tumors [NCT01848834] (43). Antibodies such as our anti-FRα clone, can also engender immune-mediated cancer cell killing via engagement of Fc receptors-expressing effector cells (monocytes, macrophages, NK cells). We exemplify these properties using patient immune effector cells *in vitro* and in orthotopic and patient-derived TNBC models *in vivo* (Fig. 5-6).

Design of anti-tumor antibodies requires selection of a target, ideally one overexpressed by cancer cells and possibly associated with engendering biological advantages to cancer. This may permit selective recognition of more aggressive cancer cells and may facilitate their destruction by targeted treatments, or engagement and activation of effector cells in the immune stroma. We provide evidence to support further evaluation of FRα as a promising target for treatment of a subset of breast cancers. We report that high FRα expression and dysregulated folate metabolic pathway may be associated with basal-like/TNBC phenotype. Importantly, FRα is expressed in high-risk high-grade disease and in post-neoadjuvant chemotherapy residual tumors, themselves associated with high metastatic relapse. Targeted therapies centered on FRα may also benefit from reported low and restricted FRα expression to a small subset of non-malignant tissues (44). We demonstrate that FRα expression confers proliferative and clonogenic advantages to tumor cells and contributes to pathway activation of Src-family non-receptor tyrosine kinases. FRα expression has been shown to associate with STAT3/JAK signaling before

16

(37), and, here in this report, to contribute to cancer cell signaling through the Src/ERK pathway. These insights point to new opportunities for targeting FRα and for disrupting its associated signaling cascades using a specific inhibitor (Fig. 3-4).

We demonstrate that FRα-expressing cells can be subjected to human volunteer and TNBC patient-derived immune cell-mediated killing with MOv18-IgG1. These effects were not seen against low FRα-expressing cells, suggesting potentially low or no on-target/off-tumor toxic effects. Lowly-expressing normal tissues, mostly rely on other routes of folate uptake, namely the reduced folate carrier or proton-coupled folate transporter. The ability of this antibody to induce ADCP/ADCC against cancer cells in an antigen-dependent manner supports continued study of this and potentially other antibody strategies as passive immunotherapies for breast tumors. Our investigations of therapeutic efficacy in orthotopic xenografts showed significant reduction in tumor growth in both TNBC line and PDTX tumors. Additionally, PDTX studies revealed an increase in tumor-infiltrating macrophages and NK cells associated with anti-FRα antibody treatment. This may suggest that targeted therapy with antibodies could present an opportunity to influence the immune stroma, enhance cancer cell recognition by effector cells and ultimately activate these cells to control tumor growth (45, 46). Our findings point to a functionally-active antibody able to prime an anti-tumor immune response that is potentially relevant and translatable to the human cancer setting.

Despite their aggressive clinical behavior, TNBCs tend to initially respond better to neoadjuvant chemotherapy compared with other breast cancer types (47). Furthermore, chemotherapeutic agents may have immunomodulatory activity within the tumor microenvironment, supporting the presence of tumor-infiltrating lymphocytes (48). However, five-year survival rates remain significantly worse in TNBC than in non-TNBC patients, likely driven by chemotherapy-resistant cells, possibly residing in micro-metastatic sites that subsequently lead to lethal clinical recurrence (35). We detected FRα-positive tumors in post-neoadjuvant treated residual TNBCs. As residual TNBCs that contain low densities of tumor-infiltrating immune cells after neoadjuvant chemotherapy have a higher risk of relapse (49), FRα-targeting antibody may present a potential strategy to retain or recruit immune effector cells in tumor stroma.

Past and ongoing clinical evaluations of FRα-targeted therapies and monoclonal antibodies, provide ground for cautious optimism. Vintafolide (MK-8109/EC145) is being evaluated in a phase III trial for ovarian cancer [NCT01170650] and a phase IIb trial for non-small cell lung cancer [NCT01577654]. A phase II trial of vintafolide in FRα-positive

17

TNBC is expected. The concept of using FRα-specific anti-folate drugs is evaluated in an early phase I trial of the first-in-class thymidylate synthase inhibitor, ONX-0801, in solid tumors [NCT02360345] (19). Furthermore, with the same specificity for an epitope of FRα, the MOv18-IgE isotype is being evaluated in a first-in-class clinical trial for ovarian cancer [NCT02546921] (50). Clinical experience with these agents points to a need for improved patient selection and for elucidating mechanisms of action. In breast cancer, FRα expression levels could be used for patient stratification. Perhaps tumor infiltration of key effector cells that may be activated against highly-aggressive or chemotherapy-resistant cancer cells, could also be employed to monitor treatment responses or to select patients more likely to benefit.

Collectively, our findings support FRα expression at the transcriptomic and protein levels, and cell surface expression in a proportion of basal-like and TNBC subtypes, including in neoadjuvant chemotherapy-resistant tumors. We report associations of higher expression with worse clinical outcomes, and evidence for functional significance in breast cancer cell biology. We demonstrate the potential tumor-restricting effects of anti-FRα MOv18-IgG1; by potentiating immune effector cell activation and cancer cell-neutralizing functions *in vitro* and by restricting tumor growth in orthotopic TNBC line and PDTX models *in vivo;* by an ADC design approach of the anti-FRα antibody coupled with a Src-family kinase inhibitor *in vitro* and *in vivo*. Our findings point to FRα as a promising antigen for different antibody therapy approaches and may provide the basis for further translational investigations, effective patient stratification and personalized therapies, especially for patients who do not adequately benefit from currently-available treatments.

18

Acknowledgments

19

References

1. Lehmann, B.D., Pietenpol, J.A. and Tan, A.R. Triple-negative breast cancer: molecular subtypes and new targets for therapy. Am Soc Clin Oncol Educ Book 2015: e31-39.

2. Perou, C.M., Sorlie, T., Eisen, M.B., van de Rijn, M., Jeffrey, S.S., Rees, C.A., et al. Molecular portraits of human breast tumours. Nature 2000; **406**: 747-752.

3. Diaz, L.K., Cryns, V.L., Symmans, F. and Sneige, N. Triple negative breast carcinoma and the basal phenotype: From expression profiling to clinical practice. Advances in Anatomic Pathology 2007; **14**: 419-430.

4. Lehmann, B.D., Bauer, J.A., Chen, X., Sanders, M.E., Chakravarthy, A.B., Shyr, Y., et al. Identification of human triple-negative breast cancer subtypes and preclinical models for selection of targeted therapies. J Clin Invest 2011; **121**: 2750-2767.

5. Baselga, J., Gomez, P., Greil, R., Braga, S., Climent, M.A., Wardley, A.M., et al. Randomized phase II study of the anti-epidermal growth factor receptor monoclonal antibody cetuximab with cisplatin versus cisplatin alone in patients with metastatic triple-negative breast cancer. J Clin Oncol 2013; **31**: 2586-2592.

6. Cameron, D., Brown, J., Dent, R., Jackisch, C., Mackey, J., Pivot, X., et al. Adjuvant bevacizumab-containing therapy in triple-negative breast cancer (BEATRICE): primary results of a randomised, phase 3 trial. Lancet Oncol 2013; **14**: 933-942.

7. Tolaney, S.M., Nechushtan, H., Ron, I.G., Schoffski, P., Awada, A., Yasenchak, C.A., et al. Cabozantinib for metastatic breast carcinoma: results of a phase II placebo-controlled randomized discontinuation study. Breast Cancer Res Treat 2016; **160**: 305-312.

8. Andre, F., Bachelot, T.D., Campone, M., Dalenc, F., Perez-Garcia, J.M., Hurvitz, S.A., et al. A multicenter, open-label phase II trial of dovitinib, a fibroblast growth factor receptor 1 (FGFR1) inhibitor, in FGFR1-amplified and nonamplified metastatic breast cancer (BC). J Clin Oncol 2011; **29**: 289.

9. Arrowsmith, J. and Miller, P. Trial watch: phase II and phase III attrition rates 2011-2012. Nat Rev Drug Discov 2013; **12**: 569.

10. Hopper-Borge, E.A., Nasto, R.E., Ratushny, V., Weiner, L.M., Golemis, E.A. and Astsaturov, I. Mechanisms of tumor resistance to EGFR-targeted therapies. Expert Opin Ther Targets 2009; **13**: 339-362.

11. Gucalp, A. and Traina, T.A. Triple-negative breast cancer: adjuvant therapeutic options. Chemother Res Pract 2011; **2011**: 696208.

12. Locasale, J.W. Serine, glycine and one-carbon units: cancer metabolism in full circle. Nat Rev Cancer 2013; **13**: 572-583.

13. Cheung, A., Bax, H.J., Josephs, D.H., Ilieva, K.M., Pellizzari, G., Opzoomer, J., et al. Targeting folate receptor alpha for cancer treatment. Oncotarget 2016; **7**: 52553-52574.

14. Hartmann, L.C., Keeney, G.L., Lingle, W.L., Christianson, T.J., Varghese, B., Hillman, D., et al. Folate receptor overexpression is associated with poor outcome in breast cancer. Int J Cancer 2007; **121**: 938-942.

15. Vergote, I., Armstrong, D., Scambia, G., Teneriello, M., Sehouli, J., Schweizer, C., et al. A Randomized, Double-Blind, Placebo-Controlled, Phase III Study to Assess Efficacy and Safety of Weekly Farletuzumab in Combination With Carboplatin and Taxane in Patients With Ovarian Cancer in First Platinum-Sensitive Relapse. J Clin Oncol 2016; **34**: 2271-2278.

16. van Zanten-Przybysz, I., Molthoff, C., Gebbinck, J.K., von Mensdorff-Pouilly, S., Verstraeten, R., Kenemans, P., et al. Cellular and humoral responses after multiple injections of unconjugated chimeric monoclonal antibody MOv18 in ovarian cancer patients: a pilot study. J Cancer Res Clin Oncol 2002; **128**: 484-492.

17. Moore, K.N., Martin, L.P., O'Malley, D.M., Matulonis, U.A., Konner, J.A., Perez, R.P., et al. Safety and Activity of Mirvetuximab Soravtansine (IMGN853), a Folate Receptor Alpha-

Targeting Antibody-Drug Conjugate, in Platinum-Resistant Ovarian, Fallopian Tube, or Primary Peritoneal Cancer: A Phase I Expansion Study. J Clin Oncol 2017; **35**: 1112-1118.

18. Luyckx, M., Votino, R., Squifflet, J.L. and Baurain, J.F. Profile of vintafolide (EC145) and its use in the treatment of platinum-resistant ovarian cancer. Int J Womens Health 2014; **6**: 351-358.

19. Tochowicz, A., Dalziel, S., Eidam, O., O'Connell, J.D., 3rd, Griner, S., Finer-Moore, J.S., et al. Development and binding mode assessment of N-[4-[2-propyn-1-yl[(6S)-4,6,7,8-tetrahydro-2-(hydroxymethyl)-4-oxo-3H-cyclopenta [g]quinazolin-6-yl]amino]benzoyl]-l-gamma-glutamyl-D-glutamic acid (BGC 945), a novel thymidylate synthase inhibitor that targets tumor cells. J Med Chem 2013; **56**: 5446-5455.

20. Kershaw, M.H., Westwood, J.A., Parker, L.L., Wang, G., Eshhar, Z., Mavroukakis, S.A., et al. A phase I study on adoptive immunotherapy using gene-modified T cells for ovarian cancer. Clin Cancer Res 2006; **12**: 6106-6115.

21. Song, D.G., Ye, Q., Poussin, M., Chacon, J.A., Figini, M. and Powell, D.J., Jr. Effective adoptive immunotherapy of triple-negative breast cancer by folate receptor-alpha redirected CAR T cells is influenced by surface antigen expression level. J Hematol Oncol 2016; **9**: 56.

22. DeRose, Y.S., Wang, G., Lin, Y.C., Bernard, P.S., Buys, S.S., Ebbert, M.T., et al. Tumor grafts derived from women with breast cancer authentically reflect tumor pathology, growth, metastasis and disease outcomes. Nat Med 2011; **17**: 1514-1520.

23. Gazinska, P., Grigoriadis, A., Brown, J.P., Millis, R.R., Mera, A., Gillett, C.E., et al. Comparison of basal-like triple-negative breast cancer defined by morphology, immunohistochemistry and transcriptional profiles. Mod Pathol 2013; **26**: 955-966.

24. The.Cancer.Genome.Atlas.Network. Comprehensive molecular portraits of human breast tumours. Nature 2012; **490**: 61-70.

25. Curtis, C., Shah, S.P., Chin, S.F., Turashvili, G., Rueda, O.M., Dunning, M.J., et al. The genomic and transcriptomic architecture of 2,000 breast tumours reveals novel subgroups. Nature 2012; **486**: 346-352.

26. Bracher, M., Gould, H.J., Sutton, B.J., Dombrowicz, D. and Karagiannis, S.N. Three-colour flow cytometric method to measure antibody-dependent tumour cell killing by cytotoxicity and phagocytosis. J Immunol Methods 2007; **323**: 160-171.

27. Matejcic, M., de Batlle, J., Ricci, C., Biessy, C., Perrier, F., Huybrechts, I., et al. Biomarkers of folate and vitamin B12 and breast cancer risk: report from the EPIC cohort. Int J Cancer 2017; **140**: 1246-1259.

28. Song, M.A., Brasky, T.M., Marian, C., Weng, D.Y., Taslim, C., Llanos, A.A., et al. Genetic variation in one-carbon metabolism in relation to genome-wide DNA methylation in breast tissue from heathy women. Carcinogenesis 2016; **37**: 471-480.

29. Rustum, Y.M., Harstrick, A., Cao, S., Vanhoefer, U., Yin, M.B., Wilke, H., et al. Thymidylate synthase inhibitors in cancer therapy: direct and indirect inhibitors. J Clin Oncol 1997; **15**: 389-400.

30. Kasoha, M., Unger, C., Solomayer, E.F., Bohle, R.M., Zaharia, C., Khreich, F., et al. Prostate-specific membrane antigen (PSMA) expression in breast cancer and its metastases. Clin Exp Metastasis 2018.

31. Sega, E.I. and Low, P.S. Tumor detection using folate receptor-targeted imaging agents. Cancer Metastasis Rev 2008; **27**: 655-664.

32. Ginter, P.S., McIntire, P.J., Cui, X., Irshaid, L., Liu, Y., Chen, Z., et al. Folate Receptor Alpha Expression Is Associated With Increased Risk of Recurrence in Triple-negative Breast Cancer. Clin Breast Cancer 2017; **17**: 544-549.

33. Zhang, Z., Wang, J., Tacha, D.E., Li, P., Bremer, R.E., Chen, H., et al. Folate receptor alpha associated with triple-negative breast cancer and poor prognosis. Arch Pathol Lab Med 2014; **138**: 890-895.

34. O'Shannessy, D.J., Somers, E.B., Maltzman, J., Smale, R. and Fu, Y.S. Folate receptor alpha

21

(FRA) expression in breast cancer: identification of a new molecular subtype and association with triple negative disease. Springerplus 2012; **1**: 22.

35. Balko, J.M., Giltnane, J.M., Wang, K., Schwarz, L.J., Young, C.D., Cook, R.S., et al. Molecular profiling of the residual disease of triple-negative breast cancers after neoadjuvant chemotherapy identifies actionable therapeutic targets. Cancer Discov 2014; **4**: 232-245.

36. Symmans, W.F., Wei, C., Gould, R., Yu, X., Zhang, Y., Liu, M., et al. Long-Term Prognostic Risk After Neoadjuvant Chemotherapy Associated With Residual Cancer Burden and Breast Cancer Subtype. J Clin Oncol 2017; **35**: 1049-1060.

37. Hansen, M.F., Greibe, E., Skovbjerg, S., Rohde, S., Kristensen, A.C., Jensen, T.R., et al. Folic acid mediates activation of the pro-oncogene STAT3 via the Folate Receptor alpha. Cell Signal 2015; **27**: 1356-1368.

38. Miotti, S., Bagnoli, M., Tomassetti, A., Colnaghi, M.I. and Canevari, S. Interaction of folate receptor with signaling molecules lyn and G(alpha)(i-3) in detergent-resistant complexes from the ovary carcinoma cell line IGROV1. J Cell Sci 2000; **113 Pt 2**: 349-357.

39. Hayes, J.M., Wormald, M.R., Rudd, P.M. and Davey, G.P. Fc gamma receptors: glycobiology and therapeutic prospects. J Inflamm Res 2016; **9**: 209-219.

40. Mozaffari, F., Lindemalm, C., Choudhury, A., Granstam-Bjorneklett, H., Lekander, M., Nilsson, B., et al. Systemic immune effects of adjuvant chemotherapy with 5-fluorouracil, epirubicin and cyclophosphamide and/or radiotherapy in breast cancer: a longitudinal study. Cancer Immunol Immunother 2009; **58**: 111-120.

41. Karagiannis, P., Gilbert, A.E., Josephs, D.H., Ali, N., Dodev, T., Saul, L., et al. IgG4 subclass antibodies impair antitumor immunity in melanoma. J Clin Invest 2013; **123**: 1457-1474.

42. Hanahan, D. and Weinberg, R.A. Hallmarks of cancer: the next generation. Cell 2011; **144**: 646-674.

43. Nanda, R., Chow, L.Q., Dees, E.C., Berger, R., Gupta, S., Geva, R., et al. Pembrolizumab in Patients With Advanced Triple-Negative Breast Cancer: Phase Ib KEYNOTE-012 Study. J Clin Oncol 2016; **34**: 2460-2467.

44. Kelemen, L.E. The role of folate receptor alpha in cancer development, progression and treatment: cause, consequence or innocent bystander? Int J Cancer 2006; **119**: 243-250.

45. Cantoni, C., Huergo-Zapico, L., Parodi, M., Pedrazzi, M., Mingari, M.C., Moretta, A., et al. NK Cells, Tumor Cell Transition, and Tumor Progression in Solid Malignancies: New Hints for NK-Based Immunotherapy? J Immunol Res 2016; **2016**: 4684268.

46. Williams, C.B., Yeh, E.S. and Soloff, A.C. Tumor-associated macrophages: unwitting accomplices in breast cancer malignancy. NPJ Breast Cancer 2016; **2.**: pii: 15025.

47. Denkert, C., von Minckwitz, G., Brase, J.C., Sinn, B.V., Gade, S., Kronenwett, R., et al. Tumor-infiltrating lymphocytes and response to neoadjuvant chemotherapy with or without carboplatin in human epidermal growth factor receptor 2-positive and triple-negative primary breast cancers. J Clin Oncol 2015; **33**: 983-991.

48. Garcia-Martinez, E., Gil, G.L., Benito, A.C., Gonzalez-Billalabeitia, E., Conesa, M.A., Garcia Garcia, T., et al. Tumor-infiltrating immune cell profiles and their change after neoadjuvant chemotherapy predict response and prognosis of breast cancer. Breast Cancer Res 2014; **16**: 488.

49. Dieci, M.V., Criscitiello, C., Goubar, A., Viale, G., Conte, P., Guarneri, V., et al. Prognostic value of tumor-infiltrating lymphocytes on residual disease after primary chemotherapy for triple-negative breast cancer: a retrospective multicenter study. Ann Oncol 2014; **25**: 611-618.

50. Josephs, D.H., Bax, H.J., Dodev, T., Georgouli, M., Nakamura, M., Pellizzari, G., et al. Anti-Folate Receptor-alpha IgE but not IgG Recruits Macrophages to Attack Tumors via TNFalpha/MCP-1 Signaling. Cancer Res 2017; **77**: 1127-1141.

Figure legends

Figure 1. Basal-like/TNBC is associated with upregulated FRα gene expression

Gene expression in METABRIC, TCGA and KCL datasets for *FOLR1, MTHFR, TYMS* and *FOLH1*. (**A**) Cohorts were divided into TNBC and non-TNBC based on IHC-defined receptor status. (**B**) Cohorts above were stratified according to PAM50 classification (Basal-like (Basal), HER2, luminal A (L.A), luminal B (L.B) and normal-like (N.L.)). Median-centered gene expression log2 values are shown. Numbers of patients per group is indicated below the graphs in the first column. *P*-values were determined using the Wilcoxon rank-sum test. (**C**) Relationship between *FOLR1* and *FOLH1* in the KCL dataset. (**D**) Association of FRα expression (upper quartile) with ten-year overall survival. (**i**) Kaplan-Meier curves in 1,402 breast cancer samples, and (**ii**) TNBC subset with 47 samples. The number of patients per group is indicated below. Significant *P*-values are indicated with an asterisk, where *$* P < 0.05; ** P < 0.005; *** P < 0.0005.$*

Figure 2. FRα expression is associated with high grade breast cancer and basal-like/TNBC, and is found in chemotherapy-resistant residual TNBC tumors.

(**A**) IHC staining for FRα membrane expression in KCL TMA. Representative images showing restricted expression in normal human kidney and lung sections, (**i**) a case with no FRα expression and negative staining, (**ii-v**) positive cell surface cancer cell FRα staining, score: 10% to 100%. Data were classified based on tumor grade and IHC- or PAM50-defined receptor status. Each group with the highest population of positive cancer cell surface staining were displayed in pie chart subdivided into three sectors (low, medium and high score based on % membrane FRα staining). (**B**) Microarray-based FRα mRNA expression were compared to membrane FRα staining positivity tested by IHC staining. (**C**) IHC staining for membrane FRα expression in KCL post-neoadjuvant chemotherapy residual TNBC tumor TMA. (**i-iv**) Representative images showing FRα staining, score: 0% to 100%. 11 out of 18 samples were found to be positive for FRα expression. Pie chart subdivided the samples into three sectors (low, medium and high score based on % of

23

cells positive for membrane FRα staining). The proportion of patients per group is indicated below. Significant *P*-value is indicated with an asterisk where *** *P < 0.0005.*

Figure 3. Surface FRα protein levels in breast cancer cell lines and RNA interference of FRα leads to reduction in cellular activities

(**A**) Surface FRα expression of twenty-two breast cancer cell lines were evaluated by flow cytometry using MOv18-IgG1. Histopathological subtype of each cell line was listed on Supplementary Fig. 2A. Cell lines with high surface FRα level that were ultimately selected for further analysis are highlighted (CAL51, red; T47D, blue; HDQ-P1, pink, also see representative histograms of flow cytometric evaluations of FRα expression). The evaluations also included the widely studied breast cancer surface receptors EGFR and HER2 as internal controls (Supplementary Fig. 2B and 2C). (**B**) FRα mRNA expression data of the cell lines were extracted from CCLE database. Analyses showed a positive correlation (r = 0.5784) between protein and mRNA levels of expression (Spearman's Rank coefficient analysis, $P < 0.01$). (**C**) Significant restrictions in cellular growth after 96 hr of siRNA-mediated silencing of FRα, and reduction in colony density over a ten-day period, were shown only in the FRα-positive cell lines. (**D**) FRα expression in CAL51 cells transduced with non-targeting shRNA (shNT) and FRα-targeting shRNA (shFRα) were represented as MFI based on MOv18-IgG1 staining. CAL51 demonstrated growth restriction, visible reduction in colony density, and decreased ERK activity with stable FRα knockdown. (**E**) Parental CAL51 were treated with raltitrexed in both normal and folate-free conditions. Cells with FRα knockdown were less sensitive to the treatment in both conditions. The data represent the mean ± SEM values of at least three independent experiments. * *P < 0.05; ** P < 0.005; *** P < 0.0005,* by two-tailed unpaired t-test.
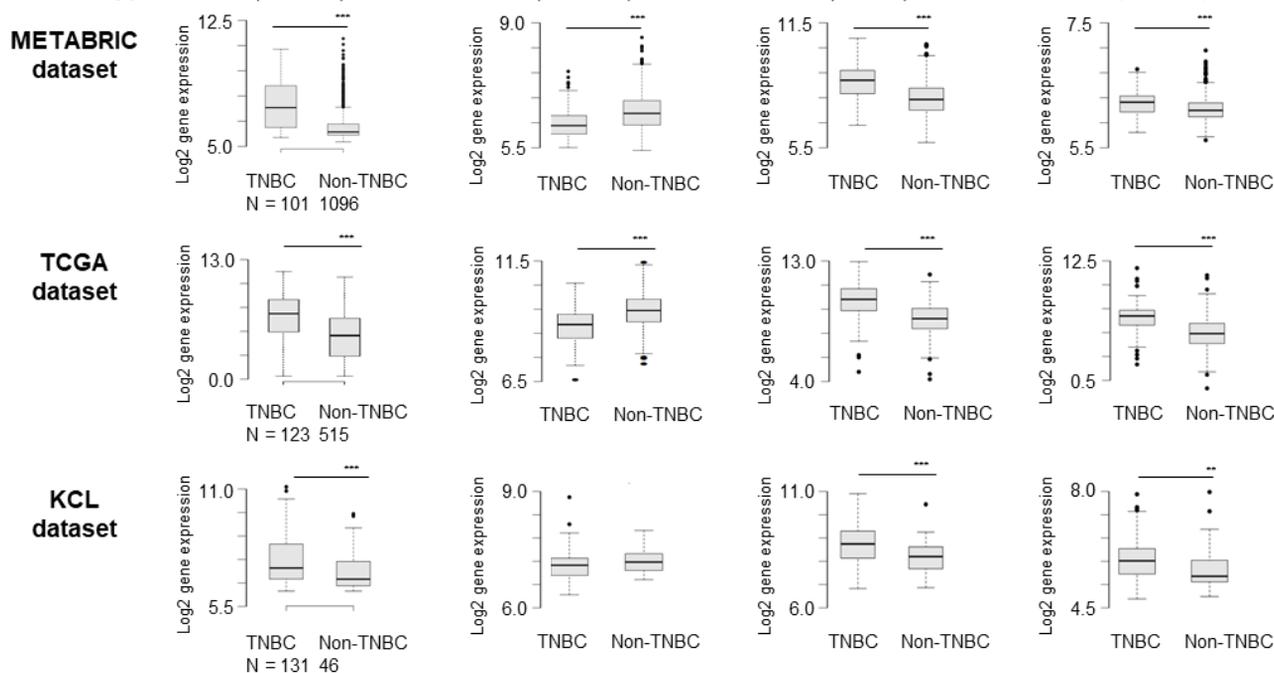

Figure 4. FRα modulates phosphorylation of targetable signaling molecules and antibody-drug conjugate inhibition of tumor growth.

(**A**) Images from Proteome Profiler Human Phospho-Kinase Array (decrease in phosphorylation marked in red; increase in phosphorylation marked in green). Each kinase is spotted in duplicate. Loading reference points at lower exposure for each membrane are shown in Supplementary Fig. 3B. Pixel densitometry analysis was expressed as fold change comparing the shFRα sample to corresponding shNT sample. (**B**) Cells were treated with board spectrum Src-family kinase inhibitor A-419259 to access the dose dependent inhibition of cellular growth. Half-maximal inhibitory concentration (IC_{50}) doses

were determined with MTT assay following 96 hr incubation. CAL51 incubated with A-419259 had shown visible reduction in colony density over a three-week period, where the inhibitor was refreshed weekly, and decreased ERK activity after 4 hr of drug treatment. (**C**) A model depicting FRα-mediated regulation of cancer signaling and as folate transporter for cell growth and survival. (**D**) Viability assessment of FRα-targeting MOv18-IgG1-coupled inhibitor ADC-treated CAL51 cells compared with MOv18-IgG1- and A-419259- treated cells. Data are means ± SEM from N = 3 independent experiments. (**E**) Growth curves and weight measurements of resected CAL51 tumors (N=10 mice per treatment group) treated with a single-dose of ADC (7.5mg/kg), MOv18-IgG1 (7.5mg/kg), A-419259 (5 mg/kg) or PBS. *P < 0.05; ** P < 0.005; *** P < 0.0005,* by two-tailed unpaired t-test.

Figure 5. MOv18-IgG1 antibody induces immunotherapeutic tumor cell killing

(**A**) Fluorescent images of the live cell cytotoxicity assay. Live CFSE-labelled CAL51 tumor cells (green) were incubated for 24 hr with MOv18-IgG1 or isotype antibody and PBMC (stained with CellTracker Blue dye). Incorporation of ethidium homodimer-1 is depicted as red fluorescence into damaged cells, was observed. (**B**) FFPE cell pellets of six breast cancer cell lines (CAL51, T47D, HDQ-P1, SKBR3, MDA-MB-231 and HCC1428) were cut and stained for evaluation of FRα expression. Breast cancer cells were treated with 5 µg/ml MOv18-IgG1, or with isotype-matched control antibody. Human U937 monocytic cells were added to the tumor cells and incubated for 3 hr at 37^oC followed by the flow cytometry-based tumor cell killing assay to determine the levels of ADCC and ADCP of cancer cells (N = 3). (**C**) Healthy volunteer PBMCs (N = 8), and TNBC patient PBMCs (N = 9) were also used, results were illustrated as total % tumor cell killing and as separated ADCC (black) and ADCP (grey). MOv18-IgG1 appeared to induce ADCP-biased anti-tumor effects. All the data represent the mean ± SEM values of three independent experiments. * *P* < 0.05; ** *P* < 0.005; *** *P* < 0.0005, by two-tailed unpaired t-test.

Figure 6. Restriction of orthotopic tumor growth *in vivo*

(**A**) IHC evaluation of FRα expression in paraffin-embedded CAL51 xenograft tumor specimens. (**B**) Tumor engraftment of human immune cells were confirmed by anti-human CD45 IHC staining in tissue sections. (**C**) Growth curves and weight measurements of resected CAL51 tumors of the partly immuno-humanized mice treated with 5 or 10 mg/kg MOv18-IgG1 antibodies. (**D**) IHC evaluation of FRα expression in a TMA of 26 PDTX

models. Representative images showing no FRα expression in KCL005 and 100% positive FRα staining in WHIM02, with 43.2% of the TNBC PDTX models (N = 26) shown to be positive of FRα expression. (**E**) Tumor engraftment of human immune cells was confirmed by anti-human CD45 IHC staining. (**F**) Growth curves and weight measurements of resected WHIM02 PDTX tumors of the partly-immuno-humanized mice treated with 10 mg/kg MOv18-IgG1. (**G**) Flow cytometric analyses demonstrating engraftment of CD45+ human immune cells in the WHIM02 PDTX model, and infiltrating immune cell populations of potential effector cells (human macrophages and NK cells). Data are means ± SEM *$P < 0.05$; ** $P < 0.005$; *** $P < 0.0005$,* by two-tailed unpaired t-test.

Figure 1

(A) IHC subtype

FRα (*FOLR1*), Methylenetetrahydrofolate reductase (*MTHFR*), Thymidylate Synthase (*TYMS*), Folate Hydrolase 1 (*FOLH1*) — METABRIC dataset, TCGA dataset, KCL dataset comparing TNBC vs Non-TNBC.

(B) PAM50 subtype

FRα (*FOLR1*), Methylenetetrahydrofolate reductase (*MTHFR*), Thymidylate Synthase (*TYMS*), Folate Hydrolase 1 (*FOLH1*) — METABRIC dataset, TCGA dataset, KCL dataset across Basal, HER2, L.A, L.B, N.L.
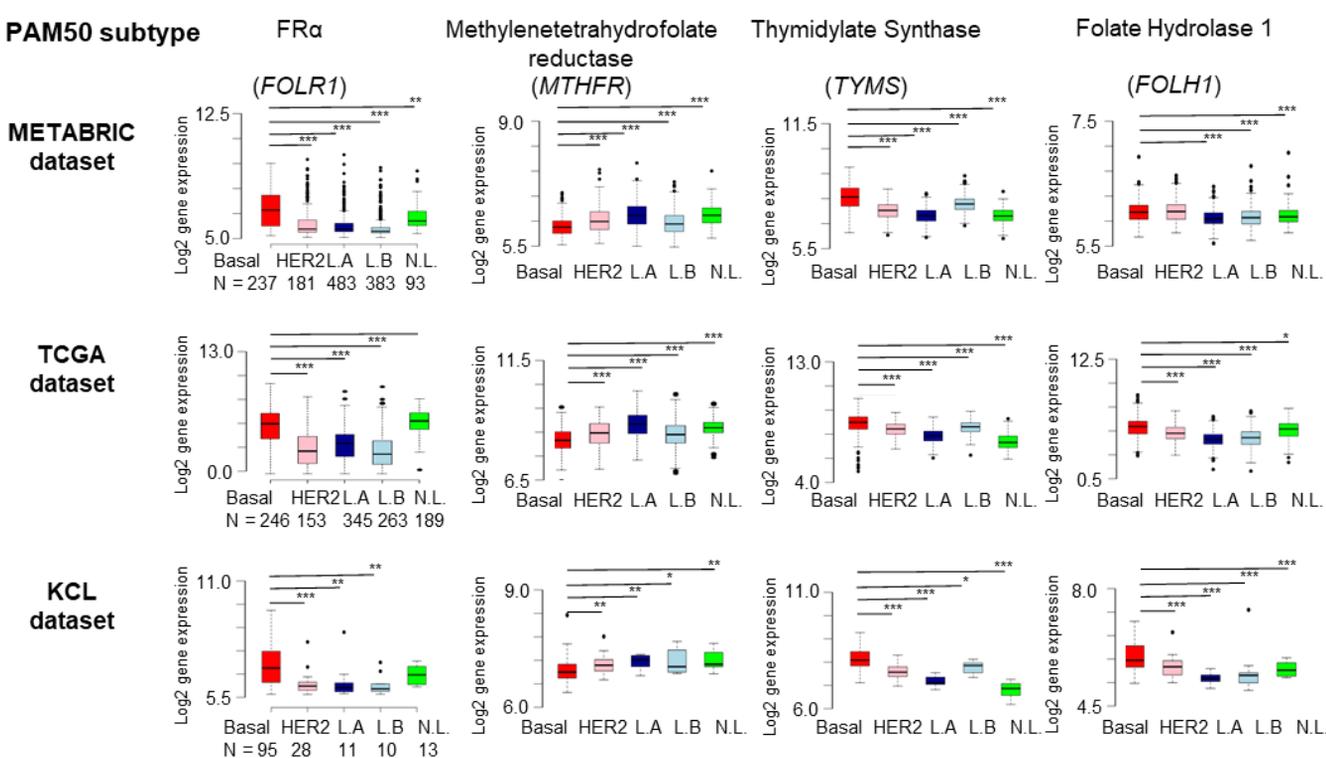
(C) FRα expression versus Folate Hydrolase 1 expression (KCL dataset N = 177)

Pearson correlation coefficient: r = 0.31
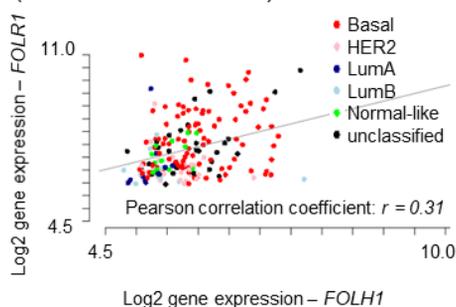
(D) Overall survival based on FRα expression (upper quartile):

(i) All breast cancer (N = 1402) — HR: 1.38 (1.08 – 1.75), P = 0.0097

(ii) TNBC (N = 47)
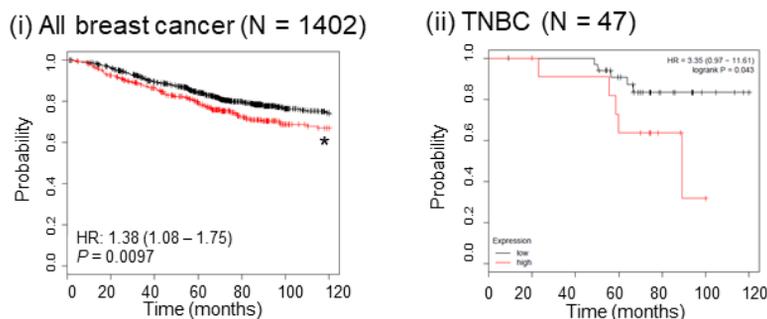
Figure 2

(A) King's College London breast cancer TMA

FRα membrane staining: % of FRα positive tumor cells

Kidney / Lung panels with scale bars 50µm, 250µm

(i) 0% (ii) 10% (iii) 45% (iv) 90% (v) 100%

Defined by grade

Grade 1 — N = 24
Grade 2 — N = 78
Grade 3 — N = 186

% of samples positive for FRα

Grade 3 membrane FRα staining (pie: High, Low, Medium)

Membrane staining
Low 10-40%
Medium 41-70%
High 71-100%

Defined by IHC

Luminal — N = 107
HER2 — N = 45
ER positive — N = 67
ER negative — N = 10
TNBC — N = 76

% of samples positive for FRα

TNBC membrane FRα staining (pie: High, Low, Medium)

Defined by PAM50

Normal-like — N = 7
Luminal B — N = 4
Luminal A — N = 14
HER2 — N = 28
Basal-like — N = 72

% of samples positive for FRα

Basal-like membrane FRα staining (pie: High, Low, Medium)

(B) Microarray-based FRα expression versus membrane FRα staining positivity (KCL basal dataset)

***

Transcriptomic FRα mRNA expression
Log2 gene expression - FRα
11.0
5.5
FRα negative / FRα positive
IHC membrane FRα staining status
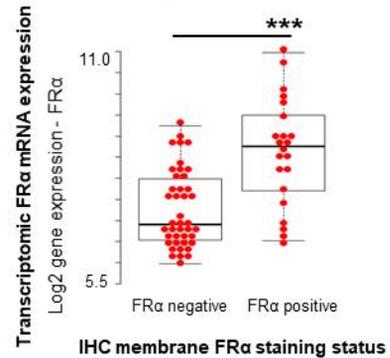
(C) King's College London TNBC residual tumor TMA

FRα membrane staining: % of FRα positive tumor cells

(i) 0% (ii) 10% (iii) 65% (iv) 90%
250µm

TNBC residual tumor TMA

Residual tumor — N = 18

% of samples positive for FRα

Residual tumor membrane FRα staining (pie: High, Low, Medium)

Membrane staining
Low 10-40%
Medium 41-70%
High 71-100%
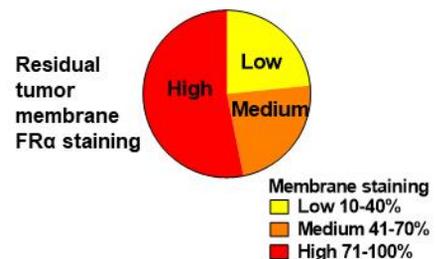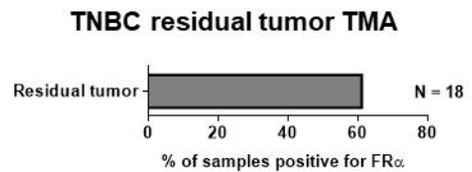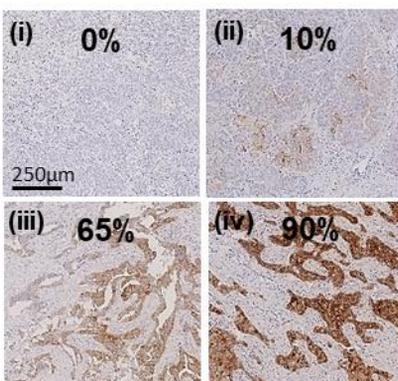
Figure 3

(A) FRα expression in breast cancer cell lines (FACS)
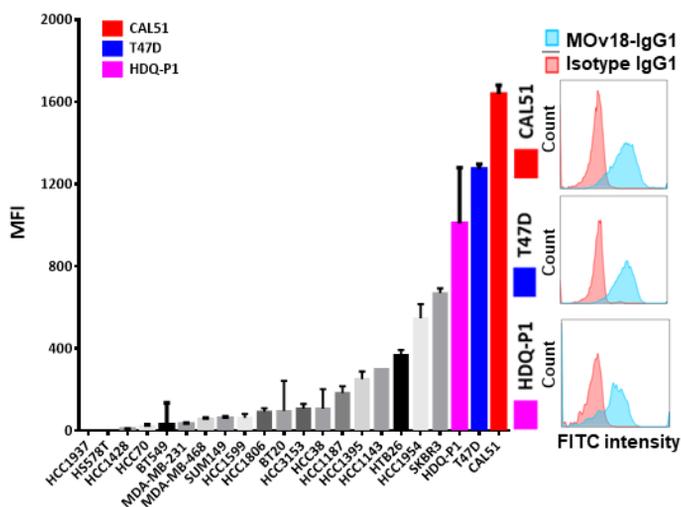
(B) FRα expression versus CCLE cell line gene expression profiles
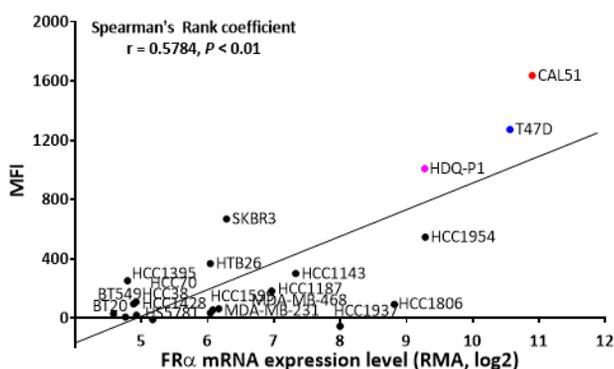
(C) siRNA knockdown - Cell viability
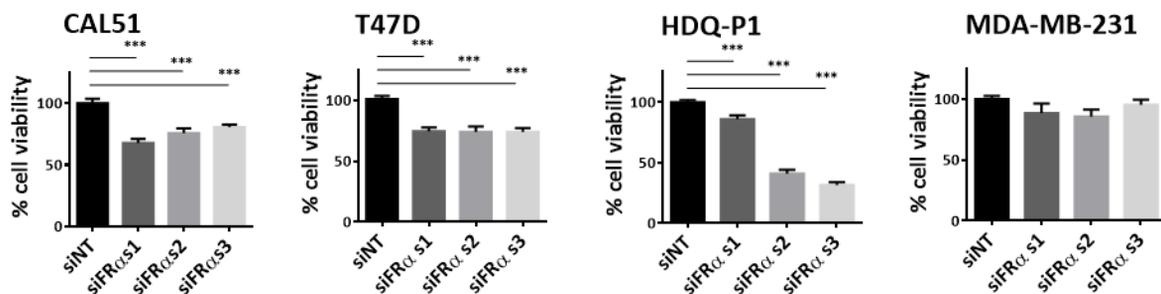
siRNA knockdown - Colony formation
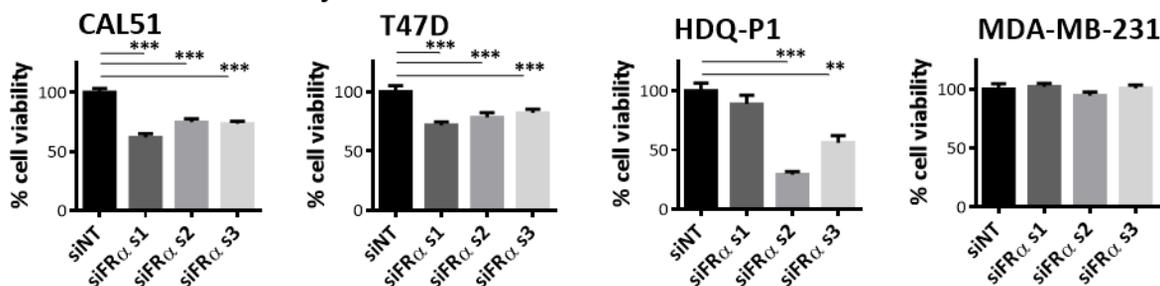
(D) shRNA knockdown in CAL51 cells
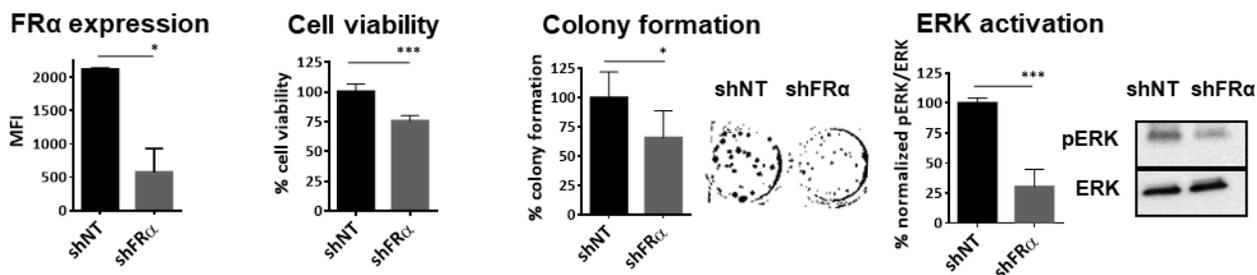
(E) Raltitrexed treatment on CAL51 cells

Raltitrexed treatment with normal growth media

Raltitrexed treatment With folate-free media
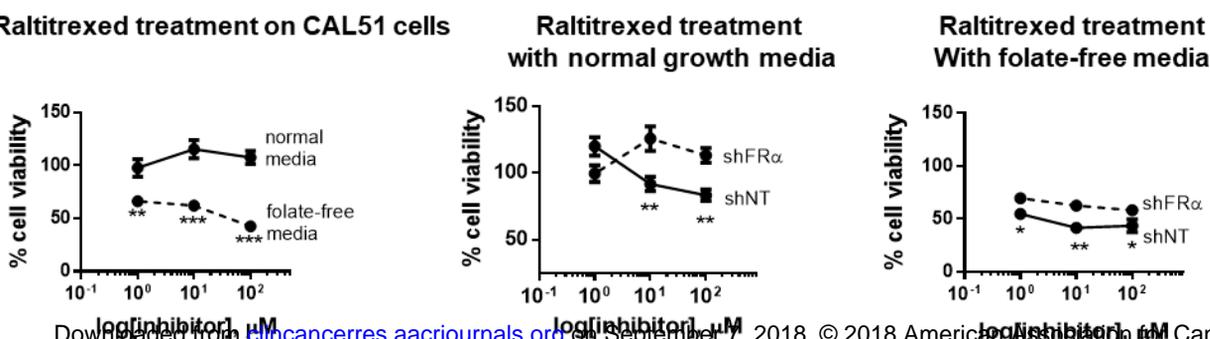
Figure 4

(A) Human Phospho-Kinase Array
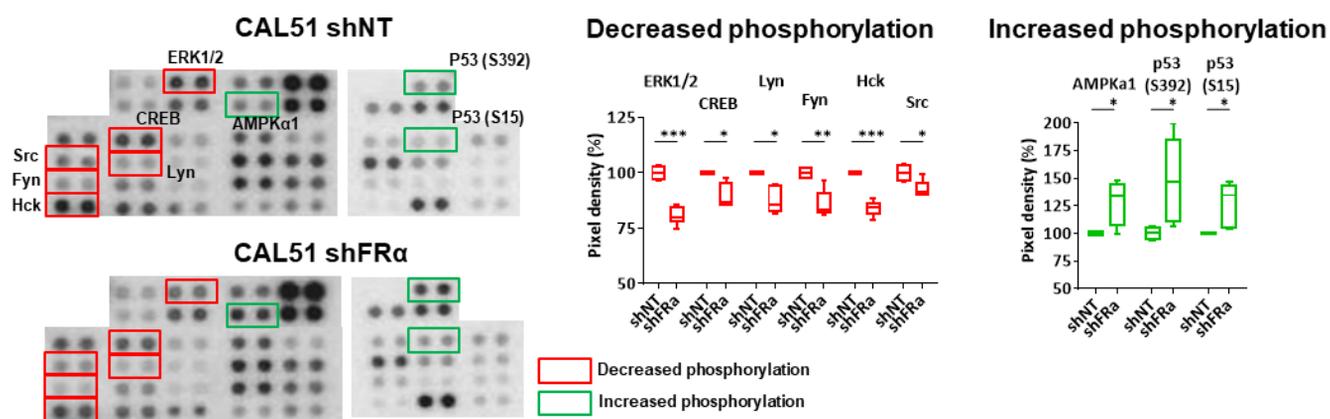
(B) Src family kinase inhibitor A-419259
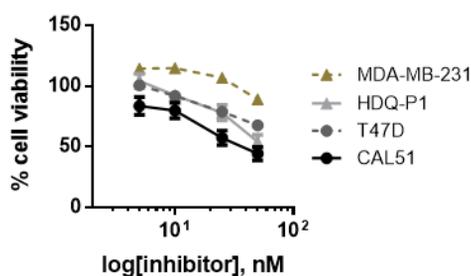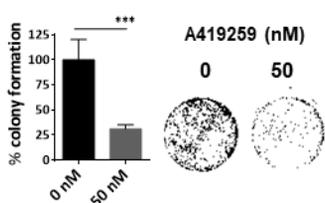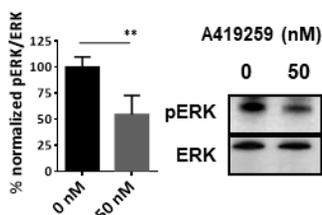
(C) FRα-mediated cancer growth
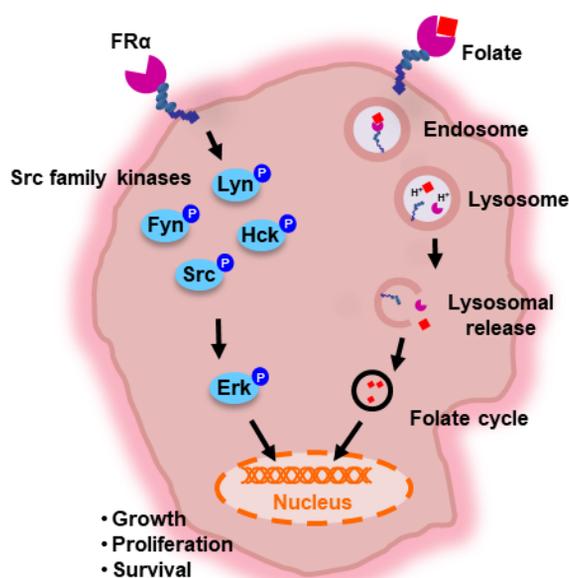
(D) Antibody-drug conjugate *in vitro* cell viability
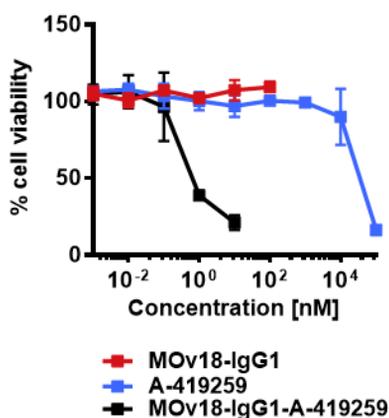
(E) Antibody-drug conjugate *in vivo* growth curve
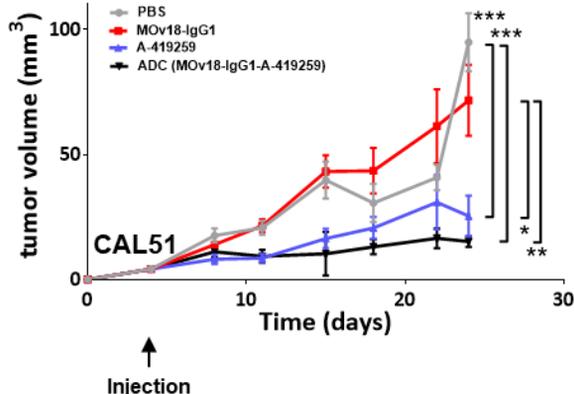
Resected tumor weight
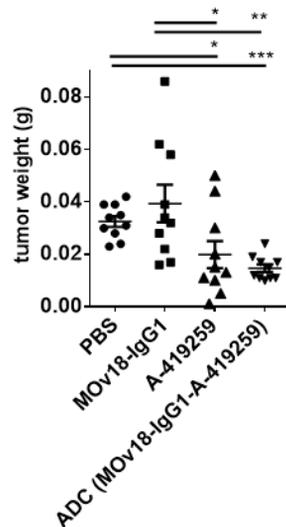
Figure 5

(A) Immunofluorescence microscopy – interaction between cancer cells and immune cells
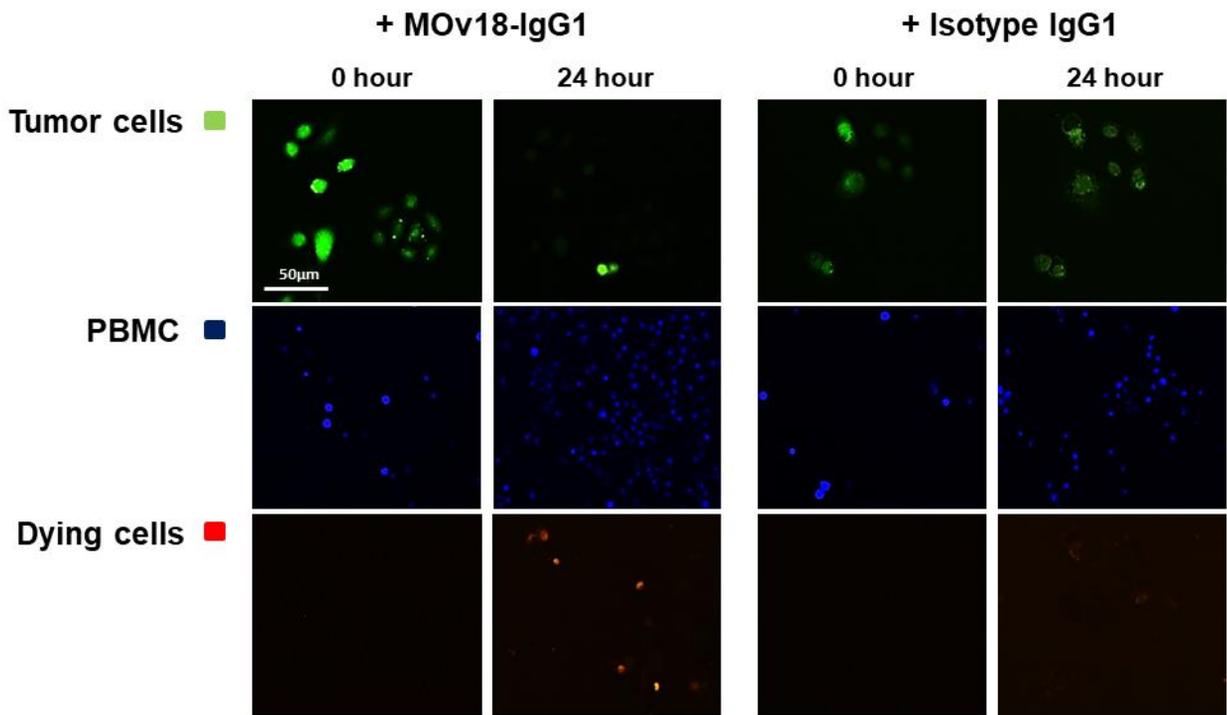
(B) FRα-dependent immune cell killing – U937 monocytic cells
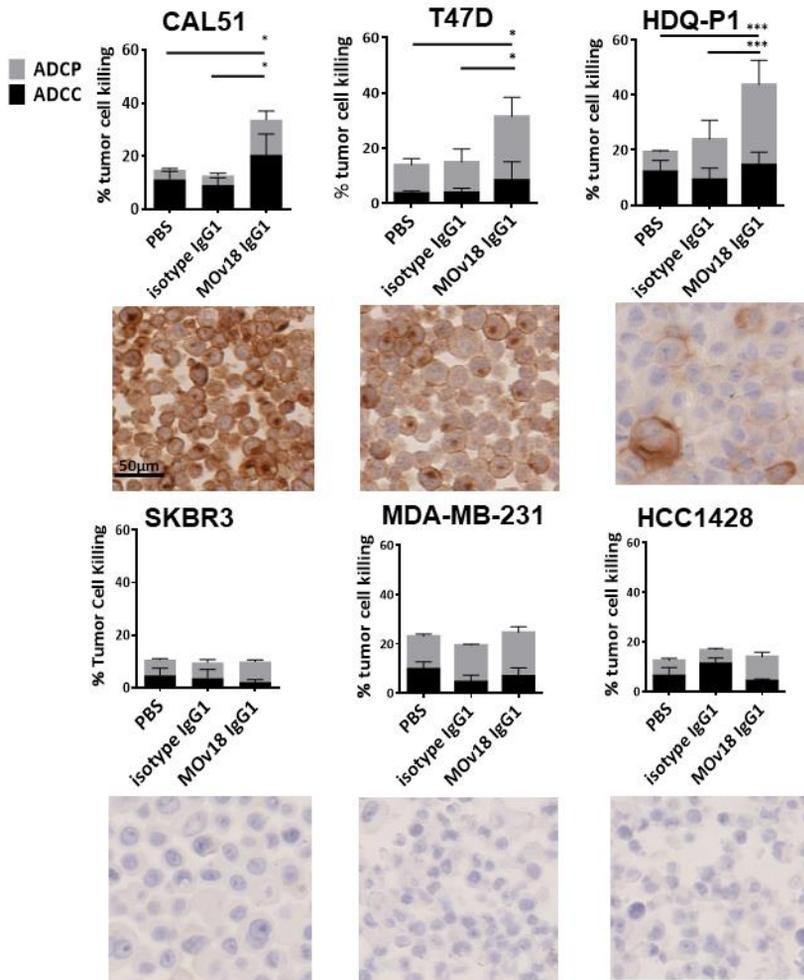
(C) Human blood sample
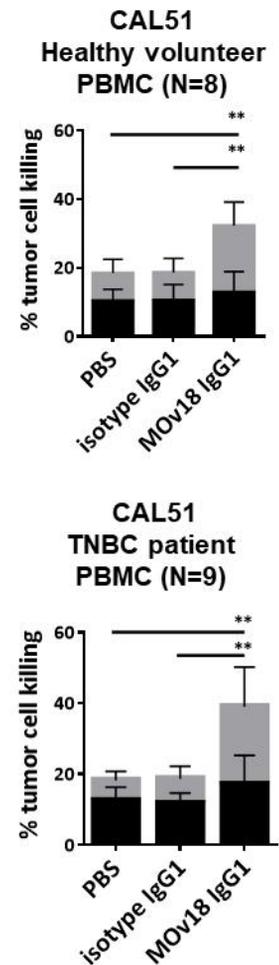
Figure 6

(A) CAL51 xenograft
FRα expression
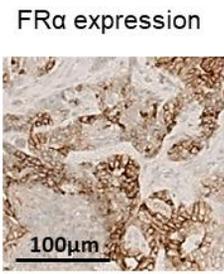
(B) CD45 IHC staining in CAL51 tumors
PBS PBS (i) / PBL PBS (ii) / PBS MOv18-IgG1 (iii) / PBL MOv18-IgG1 (iv)

(C) CAL51 growth curve
- PBS + PBS
- PBL + PBS
- PBS + MOv18-IgG1 10mg/kg
- PBL + MOv18-IgG1 5mg/kg
- PBL + MOv18-IgG1 10mg/kg
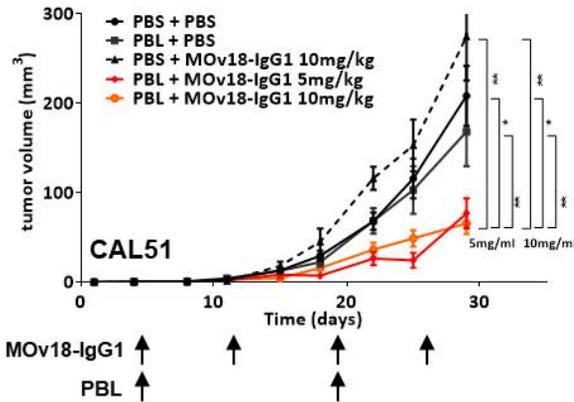
Resected tumor weight

(D) PDTX FRα membrane staining: % of FRα positive tumor cells
KCL005 / WHIM02
PDTX models N = 26
% of samples positive for FRα
PDTX models membrane FRα staining
Membrane staining
Low 10-40%
Medium 41-70%
High 71-100%

(E) CD45 IHC staining in WHIM02 tumors
PBL PBS / PBL MOv18 IgG1
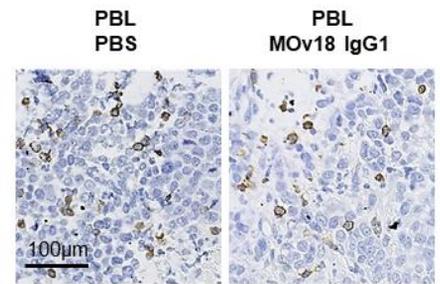
(F) WHIM02 growth curve
- PBL + PBS
- PBL + MOv18-IgG1
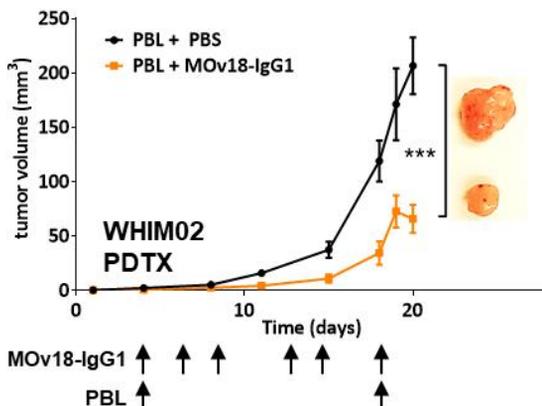
Resected tumor weight

(G) Engrafted immune cells
Total CD45+ population
Macrophage
NK cells

AACR American Association for Cancer Research
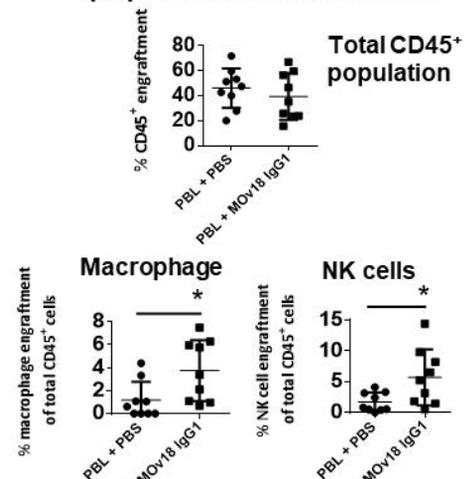
Clinical Cancer Research

Anti-Folate Receptor alpha-directed Antibody Therapies Restrict the Growth of Triple Negative Breast Cancer

Anthony Cheung, James W. Opzoomer, Kristina M Ilieva, et al.

Clin Cancer Res Published OnlineFirst August 1, 2018.